

**Picosecond ultrasonic measurements of attenuation of
longitudinal acoustic phonons in silicon**

B.C. Daly
Vassar College
Physics and Astronomy Department
Poughkeepsie, NY 12604

K. Kang, Y. Wang, and David G. Cahill
Materials Research Laboratory
Department of Materials Science and Engineering
University of Illinois
Urbana, IL 61801

Abstract

We report ultrafast optical measurements of the attenuation of 50 and 100 GHz longitudinal acoustic phonon pulses in Si. Picosecond acoustic measurements were made at temperatures $50 < T < 300$ K on thinned (50 μm thick) wafers. The measured phonon lifetimes at 300K, $\approx 5 - 7$ ns, are an order of magnitude less than expected based on three-phonon scattering rates derived from thermal conductivity data. The attenuation is instead dominated by relaxational damping. This attenuation sets an intrinsic limit on the quality factor of nanomechanical resonators that operate near room temperature.

PACS numbers: 63.20.kg, 42.65.Re, 43.58.+z

The attenuation of high-frequency acoustic waves in dielectric or semiconductor crystals is a topic with a long history that also has a critical importance to several areas of current interest in condensed matter and materials physics. First, long wavelength acoustic phonons with frequencies near 1 THz are expected to play an important role in nanoscale heat transport [1]; recent work suggests that long wavelength phonons with mean-free-paths larger than 1 μm are responsible for a significant portion of the thermal conductivity in Si at 300K [2,3]. Second, the feasibility of imaging buried nanostructures using high frequency acoustic waves will depend on attenuation levels at different temperatures and frequencies [4,5]. Finally, high quality factor nanomechanical resonators in the GHz frequency range [6,7] have potential for device applications but the intrinsic attenuation mechanisms are not yet fully understood.

Here, we report picosecond ultrasonic measurements of attenuation in a thin Si wafer in the temperature range $50 \text{ K} < T < 300 \text{ K}$ at 50 and 100 GHz. Attenuation of acoustic phonons in this frequency range in Si has been studied previously by Hao and Maris, but only at temperatures lower than 130 K [8]. The highest frequency for which the attenuation in Si has previously been measured at room temperature is 20 GHz [9]. At this frequency range, the acoustic phonon wavelength is on the order of 100 nm. This is comparable to the mean-free-paths of the higher frequency thermal phonons that are the dominant carriers of heat flow in insulating and semiconducting crystals.

In a crystalline semiconductor such as Si, the dominant mechanism for the decay of an ultrasonic wave is its interaction with thermal phonons [10]. For ultrasonic waves at high frequencies and low temperatures such that the acoustic wave frequency satisfies $\omega \sim kT/\hbar$, the attenuation is best described by three-phonon anharmonic decay processes

[11]. For lower frequency ultrasound the decay mechanism is expected to follow a relaxation damping theory due to Akhieser [12], where the sound waves disturb the occupation of thermal phonons whose frequencies depend on strain. The thermal phonons then collide with one another, returning the system to equilibrium as energy is removed from the sound wave. The frequencies studied here, while large compared with the MHz frequencies of traditional ultrasonics, are much lower than the average thermal phonon frequency which places us in a regime where either or both mechanisms could conceivably contribute to the attenuation. We further subcategorize the frequency and temperature range into the regimes $\omega\tau \gg 1$ and $\omega\tau \ll 1$ where τ is the average lifetime of the thermally excited phonons in the crystal. At lower temperatures we find ourselves squarely in the $\omega\tau \gg 1$ regime, but at room temperature where optical phonon lifetimes [13] in Si are ≈ 2 ps and acoustic phonon lifetimes are ≈ 30 ps we very nearly approach $\omega\tau = 1$.

Ultrasonic attenuation in Si due to anharmonic three phonon processes should have a quadratic dependence on frequency. An important paper by Herring [14] demonstrated that the attenuation of a phonon should vary with frequency and temperature as $\omega^a (kT / \hbar)^{5-a}$ where $a = 2$ for cubic crystals such as Si. The result holds true even at low temperatures and long wavelengths. This dependence on frequency and temperature was recently observed for 470 GHz and 940 GHz phonons in GaN [15]. In contrast, ultrasonic attenuation as described by Akhieser's relaxation damping exhibits a more complex frequency dependence, see Eq. 130 of Ref. 10. Two components of the attenuation mechanism are represented there: i) a phonon viscosity due to the Akhieser mechanism; and ii) thermoelastic damping caused by thermal conduction between

regions of differing acoustic strain. In cases where the thermoelastic damping is negligible, the attenuation α is

$$\alpha = \frac{CT}{2\rho s^3} \frac{\omega^2 \tau}{1 + \omega^2 \tau^2} (\langle \gamma^2 \rangle - \langle \gamma \rangle^2), \quad (1)$$

where C is the volumetric heat capacity, ρ is the density, s is the speed of the ultrasound wave, and γ is the Grüneisen parameter of the thermal phonons [10]. The brackets $\langle \dots \rangle$ indicate averages taken over the entire spectrum of thermally excited phonons. The attenuation should have a quadratic dependence on frequency for $\omega\tau \ll 1$ but should exhibit no frequency dependence for $\omega\tau \gg 1$. We estimate that thermoelastic damping [9] contributes an additional 10% to the Akhieser attenuation at 50 GHz and an additional 30% to the Akhieser attenuation at 100 GHz.

The samples were undoped Si [100] wafers that had been thinned to $\approx 54 \mu\text{m}$ and polished on both sides. The samples were coated with Al films ranging in thickness from 10 to 25 nm that were used as transducers. A mode-locked Ti:sapphire oscillator with a repetition rate of 80 MHz was used to perform the pump-probe experiments [16]. Both pump and probe were focused to an $8 \mu\text{m}$ $1/e^2$ radius spot on the Al film surface. The pump pulses (800 nm, ~ 200 fs, 0.2 nJ) from the oscillator rapidly heated the Al film, generating longitudinal acoustic phonon pulses through a thermoelastic effect [17]. An electro-optic modulator operating at 9.8 MHz modulated the pump beam to allow for lock-in detection. The thickness of the Si was chosen so that phonon pulses completed a single round trip through the Si in a time comparable to the 12.5 ns repetition period of the oscillator. An optical delay stage allowed detection of phonon pulses that had traveled one or two round trips through the Si [4,8,9].

Figure 1 shows the reflectivity changes $R(t)$ caused by the phonon pulses after one and two round trips at 5 temperatures ranging from 100 K to 300 K. Temperature control was provided by an optical cryostat with a cold-finger. The data were taken on a sample with a 20 nm Al film. $\Delta R(t)$ is a convolution of the amplitude of the traveling acoustic pulse and the optical sensitivity function of the Al film [17]. Each data set has been offset for clarity. To obtain the curves shown in Fig. 1, we accounted for the effects of the 9.8 MHz pump modulation. Since the modulation period is 102 ns, the phonon signal at 12.3 ns arrives roughly 45° out of phase with the lock-in reference signal. Thus, the in-phase V_{IN} and out-of-phase V_{OUT} outputs are related by $V_{IN} \approx V_{OUT} \approx V_{MAG}/\sqrt{2}$. For the signal at 24.6 ns, $V_{IN} \approx 0$ and $V_{OUT} \approx V_{MAG}$. We used the out-of-phase component of the lock-in signal and multiplied the 12.3 ns signal by $\sqrt{2}$ before representing it in Fig. 1 as a measure of $\Delta R(t)$.

The strong temperature dependence of $\Delta R(t)$ is indicated by the multiplicative factors that have been placed on the figure. While the bulk of this dependence is expected to be the temperature dependence of the acoustic attenuation, some part of it may arise from changes in the sensitivity and absorption of the Al transducer. The variation in arrival times as a function of temperature is due to the temperature dependence of the sound velocity: we find, as expected, a $\approx 0.5\%$ change in the longitudinal sound velocity between 300 K and 100 K [8,18].

Figure 2 shows Fourier transform amplitudes for the first and second pulses at 50 K for two samples: one coated with a 20 nm Al film that produced a phonon pulse with a peak at 50 GHz, and one coated with a 10 nm Al film that produced a pulse with a peak at 100 GHz. The Al film thicknesses were determined from picosecond ultrasonic

signals at short delay times (< 50 ps) [17]. Rather than treating the attenuation of each Fourier component separately [8,9], we have chosen to identify the peak frequencies of the phonon pulses generated in each sample as the frequency measured for each case.

We obtain a measurement of the attenuation α of 50 and 100 GHz phonons by analyzing the changes in the peak-to-peak amplitudes of the $\Delta R(t)$ pulses from the samples.

$$\alpha = \frac{1}{d} \ln \left(\frac{|\Delta R_1|}{|\Delta R_2|} \right), \quad (2)$$

where d is the round trip distance through the Si wafer and the peak-to-peak amplitudes of the pulses detected after one and two round trips in the Si wafer are given by ΔR_1 and ΔR_2 . This simple analysis ignores any possible extrinsic losses such as those due to surface scattering. To account for these effects, we measured the samples down to $T \leq 50$ K and obtained results such as those illustrated in Fig. 3 for the 20 nm film sample (peak Fourier amplitude of 50 GHz) in the temperature range $25 \text{ K} < T < 300 \text{ K}$. The attenuation obeys a $T^{2.5}$ dependence between 200 K and 300 K but levels off below 100 K. The low temperature limit of the data is therefore a measure of acoustic attenuation that is not intrinsic to Si and is most likely dominated by interfacial losses at the Al/Si interface or the Si/vacuum interface at the backside of the sample. This temperature independent offset in the attenuation is equivalent to 51 cm^{-1} for the 20 nm film sample. Thus, the intrinsic component of α for Si [100] is measured to be $138 \text{ cm}^{-1} - 51 \text{ cm}^{-1} = 87 \text{ cm}^{-1}$ at 300K. Similar analysis of the 10 nm film sample that produced 100 GHz pulses yields an attenuation of 119 cm^{-1} at 300 K, a 37% increase over the attenuation of the 50 GHz pulses.

An important result of this work is the determination of the lifetimes of long-wavelength acoustic phonons. From $\tau_{ACOUSTIC} = (2\alpha s)^{-1}$ we find a phonon lifetime of 6.8 and 5.0 ns for 50 GHz and 100 GHz longitudinal acoustic phonons, respectively, at room temperature. These values are significantly shorter than the value obtained by extrapolating the lifetimes of higher frequency phonons obtained from thermal conductivity data. In Fig. 4a, we plot our measured values for the phonon lifetimes versus frequency at 300 K alongside lines representing two calculations of phonon lifetime and lifetimes determined from previous attenuation measurements [19,20,21,9]. The line labeled TC in Fig. 4a is the function $\tau_{AC.} = (B\omega^2 T)^{-1}$; the coefficient $B = 2.4 \times 10^{-19} \text{ s K}^{-1}$ describes the rate of phonon scattering by normal processes [22]. This function overestimates the lifetime by a factor of 20 for 50 GHz and a factor of 8 for 100 GHz phonons. Relaxation damping, i.e., α given by Eq. 1, is in much better agreement with our data and previously published results near 1 GHz, see Fig. 4a. To calculate the relaxation damping, we have assumed that, since the Gruneisen parameter for Si varies with mode and frequency from slightly less than -1 to slightly more than +1, we can treat the factor in the parenthesis in Eq. 1 as ≈ 1 . We used a value for the thermal phonon lifetime $\tau = 17 \text{ ps}$, which provided the best fit to the 50 GHz and 100 GHz data.

Our characterization of the relaxational phonon damping rate in Si impacts current research on heat transport in nanostructures [2]—which requires a thorough understanding of the distribution of phonon mean-free-paths for phonon—and studies of thermoelectric energy conversion where the enhancements of thermoelectric performance due to ‘phonon drag’ effect [23] depend on the relative strengths of electron-phonon and phonon-phonon scattering. Our results also have a critical relevance to the emerging

field of high-Q, high frequency nanomechanical resonators. While surface losses are thought to play a dominant role in the damping of high-frequency modes in nanometer scale electromechanical systems [7], our measurements show that intrinsic losses will contribute significantly as higher frequency resonators are investigated. Figure 4b is a second view of the results shown in Fig. 4a which plots the ideal quality factor versus frequency for a longitudinal resonator made from Si. The region of weak frequency dependence of acoustic phonon lifetime that is indicated by our measurements implies that there is a minimum in the ideal Q factor as a function of frequency where $\omega\tau \approx 1$. Beyond this minimum there should then be a small region in the sub-THz range where the ideal Q-factor would increase, until the point where three-phonon processes take over and the lifetime decreases as ω^2 .

In summary, we have used picosecond ultrasonics to measure the attenuation of longitudinal acoustic phonons in Si at 50 GHz and 100 GHz. The lifetime of these phonons is determined to be roughly an order of magnitude lower than is predicted from thermal conductivity measurements. The magnitude and frequency dependence of the attenuation is consistent with relaxation damping. Our results indicate that intrinsic relaxational loss mechanisms will play a role in the Q-factor of nanomechanical resonators in the GHz regime.

This work was partially supported by NSF Awards DMR-0605000, DMR-0906753 and by the U.S. DOE, Division of Materials Sciences under Award No. DE-FG02-07ER46459, through the Frederick Seitz Materials Research Laboratory (FSMRL) at the University of Illinois at Urbana-Champaign. The work was carried out in part in the

FSMRL Central Facilities, which are partially supported by the DOE under grants DE-FG02-07ER46453 and DE-FG02-07ER46471.

REFERENCES

- [1] D.G. Cahill, et. al., J. Appl. Phys. **93**, 793 (2003).
- [2] A.S. Henry and G. Chen, J. Comp. Theor. Nanoscience **5**, 1 (2008).
- [3] D.A. Broido, M. Malorny, G. Birner, N. Mingo, and D.A. Stewart, Appl. Phys. Lett. **91**, 231922 (2007).
- [4] B.C. Daly et al., Appl. Phys. Lett. **84**, 5180 (2004).
- [5] S. Ramanathan and D.G. Cahill, J. Mater. Res. **21**, 1204 (2006).
- [6] R. Lifshitz and M.L. Roukes, Phys. Rev. **B 61**, 5600 (2000).
- [7] K.L. Ekinici and M.L. Roukes, Rev. Sci. Inst. **76**, 061101 (2005).
- [8] H.Y. Hao and H.J. Maris, Phys. Rev. **B 63**, 224301 (2001).
- [9] J.-Y. Duquesne and B. Perrin, Phys. Rev. **B 68**, 134205 (2003).
- [10] H.J. Maris in *Physical Acoustics*, edited by W.P. Mason and R.N. Thurston, (Academic Press, New York, 1971), Vol. 8, p. 279.
- [11] L. Landau and G. Rumer, Phys. Z. Sowjetunion **11**, 18 (1937).
- [12] A. Akhieser, J. Phys. (USSR) **1**, 277 (1939).
- [13] Jeffrey J. Letcher, Kwangu Kang, David G. Cahill, and Dana D. Dlott, Appl. Phys. Lett. **90**, 252104 (2007).
- [14] C. Herring, Phys. Rev. **95**, 954 (1954).
- [15] T.-M. Liu et. al., Appl. Phys. Lett. **90**, 041902 (2007).
- [16] R.M. Cotescu, M.A. Wall, and D.G. Cahill, Phys. Rev. **B 67**, 054302 (2003).
- [17] C. Thomsen, H.T. Grahn, H.J. Maris, and J. Tauc, Phys. Rev. **B 34**, 4129 (1986).
- [18] H.J. McSkimin, J. Appl. Phys. **24**, 988 (1953).
- [19] K.R. Keller, J. Appl. Phys. **38**, 3777 (1967).

- [20] A.A. Bulgakov, V.V. Tarakanov, and A.N. Chernets, *Sov. Phys. Solid State* **15**, 1280 (1973).
- [21] Y.V. Ilisavski and V.M. Sternin, *Sov. Phys. Sol. State* **27**, 236 (1985).
- [22] D. G. Cahill, F. Watanabe, A. Rockett, and C.B. Vining, *Phys. Rev. B* **71**, 235202 (2005).
- [23] P.G. Klemens in *Proceedings of the 15th International Conference on Thermoelectrics* (IEEE, Piscataway, NJ) p. 206.

FIGURE CAPTIONS

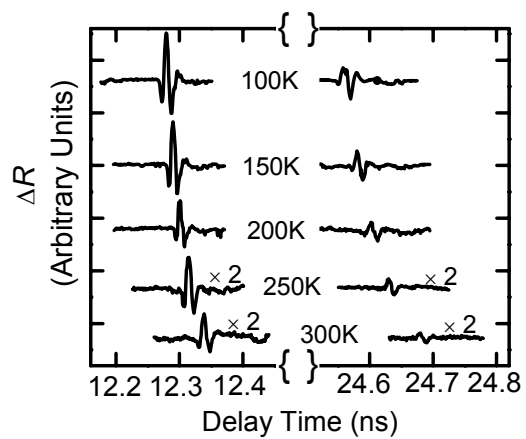
FIG. 1. $\Delta R(t)$ for a 20 nm Al film sample. Phonon pulses are shown after one (12.3 ns) and two (24.6 ns) round trips in the Si wafer. The signals at 250 and 300 K are multiplied by a factor of two to allow visual comparison.

FIG. 2. Fourier transforms of ΔR at 50 K for two samples. The '100 GHz' plots signals from a 10 nm film sample and the '50 GHz' plots represent the signals from a 20 nm film sample. The data have been rescaled so that the magnitudes of the 1st round trips are the same.

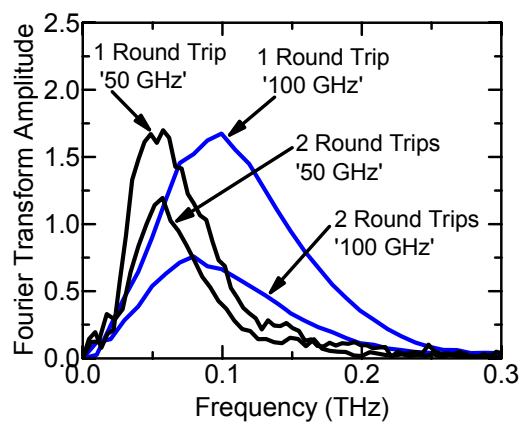
FIG. 3. Peak-to-peak amplitudes of the 1st (■) and 2nd (●) ΔR pulses for the 20 nm Al film (50 GHz) sample.

FIG. 4. **(a)** Phonon lifetime versus frequency in Si at 300K. The (■) represent our measured values of the lifetime of 50 GHz and 100 GHz longitudinal acoustic phonons. Uncertainty was estimated by an analysis of two samples with peak frequency ≈ 50 GHz. The (○),(×),(●), and (▲) represent Ref. 8, Ref. 19, Ref. 20, and Ref. 21 respectively. Data from Ref. 20 is for [111] Si. The line labeled TC represents $\tau_{AC} = (B\omega^2T)^{-1}$ with $B = 2.4 \times 10^{-19} \text{ s K}^{-1}$. The line labeled RD represents τ_{AC} based on α calculated using Eq. 1 with $\tau = 17$ ps. **(b)** Ideal quality factor $Q = f\tau$ for a nanomechanical resonator based on the data shown in part (a).

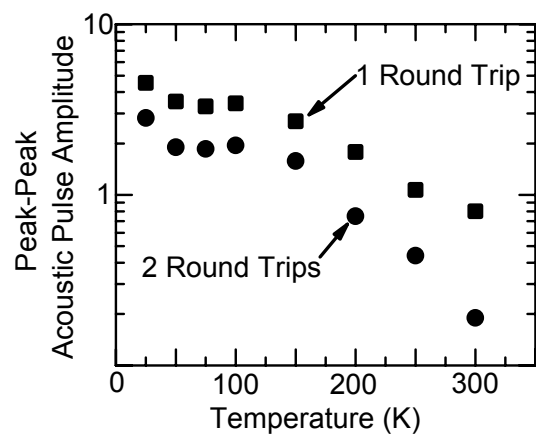
DALY, KANG, WANG, AND CAHILL FIGURE 1



DALY, KANG, WANG, AND CAHILL FIGURE 2

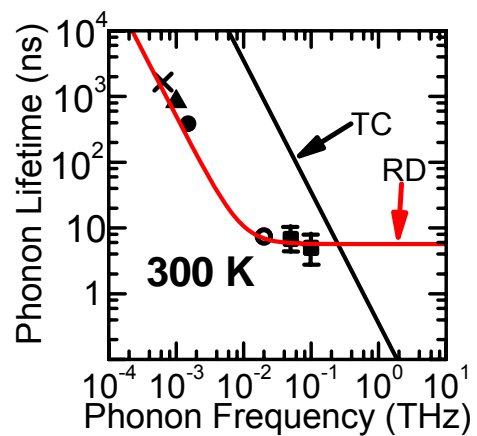


DALY, KANG, WANG, AND CAHILL FIGURE 3



DALY, KANG, WANG, AND CAHILL FIGURE 4

(a)



(b)

